Proceedings of ALGORITMY 2024
pp. 264–273

DICTIONARY LEARNING WITH THE K-SVD ALGORITHM FOR RECOVERY OF HIGHLY TEXTURED IMAGES –AN EXPERIMENTAL ANALYSIS–

ALEXANDER KÖHLER , MICHAEL BREUß , AND SHIMA SHABANI

Abstract. Image recovery by dictionary learning is of potential interest for many possible applications. To learn a dictionary, one needs to solve a minimization problem where the solution should be sparse. The K-SVD formalism, which is a generalization of the K-means algorithm, is one of the most popular methods to achieve this aim. We explain the preprocessing that is needed to bring images into a manageable format for the optimization problem. The learning process then takes place in terms of solving for sparse representations of the image batches. The main contribution of this paper is to give an experimental analysis of the recovery for highly textured imagery. For our study, we employ a subset of the Brodatz database. We show that the recovery of sharp edges plays a considerable role. Additionally, we study the effects of varying the number dictionary elements for that purpose.

Key words. Image recovery, dictionary learning, sparse representation, textured images

AMS subject classifications. 94A08, 65K05

1. Introduction.

Motivated by studying information processed in the primary visual cortex, Field and Olshausen [14] developed a first approach to sparse dictionary learning. Technically, sparse dictionary learning is a representation learning method that aims at finding a sparse representation of input data. This is done in terms of a linear combination of basic elements called atoms. The aim of dictionary learning is to find the basic elements themselves, relying on given training data, as well as finding a useful linear combination of them. Typically, the elements of the dictionary do not make up an orthogonal basis. It is often of interest to have an overcomplete dictionary with significantly more elements than the dimensionality of the input data encourages. The representation of input data in terms of the overcomplete dictionary may be more sparse than if we had just enough elements to span the space.

In this paper, we deal with textured images as input data. For possible dictionaries in image processing, one may either employ a predefined dictionary using for example wavelets for construction, or learn it at hand of the given imagery. As indicated, we pursue the latter approach, which has lead to state-of-the-art results in many applications, for example denoising [10], image deblurring [13, 17], or image segmentation [6]. We refer to [7, 18] for more information and recent applications.

Let us turn to the learning process. We describe the dictionary in terms of a matrix $D \in \mathbb{R}^{n\times K}$, where $K \gg n$ so that the dictionary will be overcomplete. Thereby the atoms are the columns, and one may refer to D in terms of the atoms as $\{d_i\}_{i=1}^K$ with $d_i \in \mathbb{R}^n$. We assume that a training database $\{y_i\}_{i=1}^N$ with $y_i \in \mathbb{R}^n$ is given. Let us put together the y_i into a training matrix $Y \in \mathbb{R}^{n\times N}$, and define a sparse representation matrix $X \in \mathbb{R}^{K\times N}$. The core idea is to find the dictionary D and the sparse representation matrix X such that $Y \approx DX$. This may be considered as a specific matrix decomposition of the training matrix. Finding the approximate decomposition in terms of a dictionary matrix and a sparse representation matrix is a minimization problem with two stages: dictionary updating and sparse coding.

Various methods deal with these two stages in different ways, see e.g. [7]. Among

them, the K-SVD algorithm [2] is one of the most popular methods for dictionary learning. It is a generalization of the K-means algorithm [9], combined with a step that performs the singular value decomposition (SVD) to update the atoms of the dictionary one by one. Besides, it enforces encoding of each input data by a linear combination of a limited number of non-zero elements. In the Section 2, we discuss the K-SVD method in some more detail.

Related work. Let us focus here on some important methods that are technically related to the K-SVD method and may be seen as extensions of the work [14]. The method of optimal directions (MOD) [8] is one of the first methods introduced to tackle the sparse dictionary learning problem. Its key idea is to solve the arising minimization problem in the sparse coding stage by enforcing a limited number of contributions of each atom in the training set. Concerning the latter point, let us note that the K-SVD method employs a similar approach. The algorithm in [12] is a process for learning an overcomplete basis by viewing it as a probabilistic model of the observed data. This method can be viewed as a generalization of the technique of independent component analysis, which is technically related to the SVD. The method in [11] proposes to learn a sparse overcomplete dictionary as unions of orthonormal bases. The dictionary update of one chosen atom is performed using SVD. Let us note that K-SVD follows a similar approach.

There have been general experimental evaluations of the overall usefulness of the K-SVD method in dictionary learning [2], see also theoretical discussions, e.g. [3].

Our contribution. In this paper, we give a dedicated experimental analysis of the K-SVD algorithm in its ability to recover highly textured images. Such images impose the challenges that their content is often not smooth and there are many fine structures that need to be recovered. Our investigation is motivated by ongoing research in corresponding applications.

2. Sparse Dictionary Learning and K-SVD Algorithm. As indicated, in sparse dictionary learning, the atoms $\{d_i\}_{i=1}^K$ yield an overcomplete spanning set and provide an improvement in the sparsity and flexibility of the input data representation.

The sparse representation x of an input y may be exact or approximate in terms of the dictionary D. The general form of the model for exact representation in sparse coding amounts to solve

$$\min_x \|x\|_0 \quad \text{w.r.t.} \quad y = Dx \tag{2.1}$$

while for the approximate representation we refer to

$$\min_x \|x\|_0 \quad \text{w.r.t.} \quad \|y - Dx\|_2 \leq \epsilon \tag{2.2}$$

Thereby $\|\cdot\|_0$ counts the non-zero entries of a vector, $\|\cdot\|_2$ stands for the Euclidean norm; the known parameter ϵ is a tolerance for the sparse representation error.

Turning now concretely to the optimization of the learning process based on the training database $\{y_i\}_{i=1}^N$, the aim is to estimate $D \in \mathbb{R}^{n\times K}$ with atoms $\{d_i\}_{i=1}^K$ and $X \in \mathbb{R}^{K\times N}$ with columns $\{x_i\}_{i=1}^N$, such that

$$\min_{D,\, x_i} \sum_{i=1}^N \|x_i\|_0 \quad \text{w.r.t.} \quad \|y_i - Dx_i\|_2^2 \leq \epsilon \tag{2.3}$$

Solving (2.3) for each $y_i \in \mathbb{R}^n$ gives a sparse representation $x_i^{\text{opt}} \in \mathbb{R}^K$ over the unknown dictionary D, aiming to find the proper sparse representations and the dictionary *jointly*. Thus, (2.3) encompasses both sparse coding and dictionary updating.

One may also consider the alternative form of (2.3) as

$$\min_{D,\,x_i} \sum_{i=1}^{N} \|y_i - Dx_i\|_2^2 \quad \text{w.r.t.} \quad \|x_i\|_0 \leq T \tag{2.4}$$

where the role of the penalty and the constraint are reversed, and the parameter T controls the number of non-zero elements in the vector.

Let us now turn to the main algorithm of the paper. As the K-SVD method is a generalization of the K-means method, we begin by a brief explanation of the latter before discussion of K-SVD.

2.1. The K-means Algorithm. There is a relation between sparse representation and clustering [8, 16]. The K-means method is a possible approach to clustering which aims to partition N inputs into K clusters, and each input belongs to the cluster with the nearest mean. The cluster centres serve as a prototype of the cluster.

The K-means method amounts to an iterative process incorporating two steps per iteration. For convenience, let us also relate to corresponding steps in dictionary learning. First, given $\{d_i\}_{i=1}^K$, it assigns the training samples ($\{y_i\}_{i=1}^N$) to their nearest neighbour in terms of the d_i (sparse coding). This means, the d_i have the role of the closest cluster centroid. Let us note that in standard K-means this is done regarding the squared Euclidean distance, while in K-SVD [2] the non-squared Euclidean distance is employed, mimicking the sparse coding problem setup. Then, the dictionary $\{d_i\}_{i=1}^K$ is updated to better fit the samples by use of the assignment given in the first step (dictionary update).

More precisely, in the sparse coding stage the method makes K partitions (subsets) of the training samples $\{y_i\}_{i=1}^N$, related to K columns of the dictionary, each holding training samples most similar to the corresponding column. At the dictionary updating stage, each dictionary column is replaced by the centroid of the corresponding subset. Let us note that K is a parameter that needs to be specified.

2.2. The K-SVD Algorithm . The essence of the iterative K-SVD algorithm, as a generalization of K-means, may be described as follows. First, the dictionary is fixed to find the best possible sparse matrix representation X under the constraint in (2.4). Then the atoms of the dictionary D are updated iteratively to better fit to the training data. This is done specifically by finding a rank-1 approximation of a residual matrix via making use of the SVD while preserving the sparsity.

One may view the problem posed in (2.4) as a nested minimization problem, namely an inner minimization of the number of non-zeros in the representation vectors x_i for a given fixed D (sparse coding stage) and an outer minimization over D (dictionary update stage). At the jth step, obtaining a sparse representation via a pursuit algorithm [7] such as e.g. orthogonal matching pursuit, for implementation details see [15], we use the dictionary D_{j-1} from the $(j-1)$th step and solve N instances of (2.4) for each y_i. That gives us the matrix X_j containing columnwise all sparse representations (sparse representation matrix). Summarizing thus the squared Euclidean norms of vectors in (2.4) using the Frobenius norm, we solve for D_j in terms of the following least squares problem, the solution of which has an exact representation:

$$D_j = \arg\min_D \|Y - DX_j\|_F^2 = YX_j^T(X_jX_j^T)^{-1} \tag{2.5}$$

The K-SVD method handles the atoms in D sequentially. Keeping all the columns fixed except the i_0th one, (d_{i_0}), it updates d_{i_0} along with the coefficients that multiply

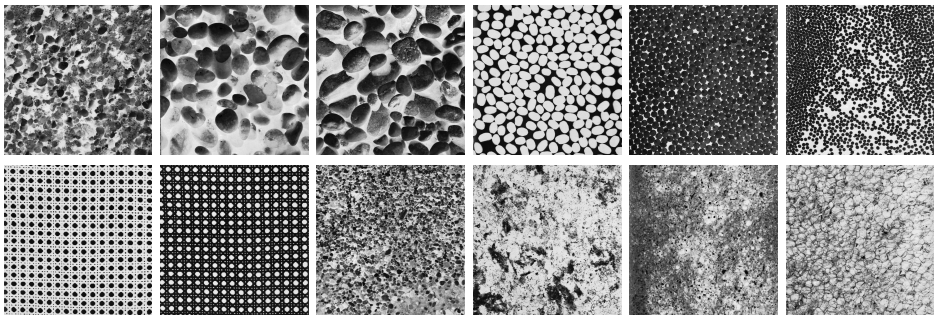

Fig. 3.1: Our considered selection of the Brodatz database [1]. From left to right and top to bottom, we used the images with the name: D27, D30, D31, D75, D66, D67, D101, D102, D54, D60, D73 and D112.

it in the sparse representation matrix. To this end, we may rewrite the penalty term in (2.5), omitting the iteration number j, as

$$\|Y - DX\|_F^2 = \Big\|Y - \sum_{i=1}^{K} d_i x_i^r\Big\|_F^2 = \big\|E_{i_0} - d_{i_0} x_{i_0}^r\big\|_F^2 \tag{2.6}$$

to isolate the dependency on d_{i_0}. Here, $E_{i_0} = Y - \sum_{i \neq i_0} d_i x_i^r$ is a precomputed residual matrix and x_i^r stands for the row r of X, so that x_i^r indicates the contribution of d_i in the training set. Which means it includes sparse coefficients of elements of the training set that currently use d_i.

The optimal values of d_{i_0} and $x_{i_0}^r$ minimizing (2.6) are given by the rank one approximation of E_{i_0}, which one can obtain using the SVD. That typically would yield a dense vector $x_{i_0}^r$, increasing the number of non-zeros in X. Keeping the cardinalities of all the representations fixed during the minimization, one may restrict E_{i_0} to those columns where the entries in the row $x_{i_0}^r$ are non-zero. In this manner, only the existing non-zero coefficients in $x_{i_0}^r$ may vary, preserving in this way the sparsity.

Considering the SVD of the restricted E_{i_0} as $E_{i_0}^R = U\Sigma V$, the updated dictionary column is the first column of U, and the updated non-zero coefficient of $x_{i_0}^r$ is the first column of V multiplied by $\Sigma(1,1)$. The K-SVD algorithm performs an SVD for each of the K different residuals related to the K columns of the dictionary. This method is a direct generalization of the K-means process. When the model orders $T = 1$ in (2.4), K-SVD exactly acts like K-means [2].

3. Data Set of Textured Images and Preprocessing. In this section, we want to explain which data set we consider, which transformation process is applied to the data set, and how we learn the dictionary.

Our experiments are based on a subset of the Brodatz texture database [5] obtained via the website [1], see Fig. 3.1. The complete data set contains 112 highly textured gray scale images with a resolution of 640×640 pixels. For our study, we select images with a dot-like texture.

3.1. Preprocessing. We begin by describing the basic steps to transform the resource images I_{orig} into a useful format. In doing this, we mostly follow the basic steps of the Matlab code [4], which is the source of our computation, too. The use

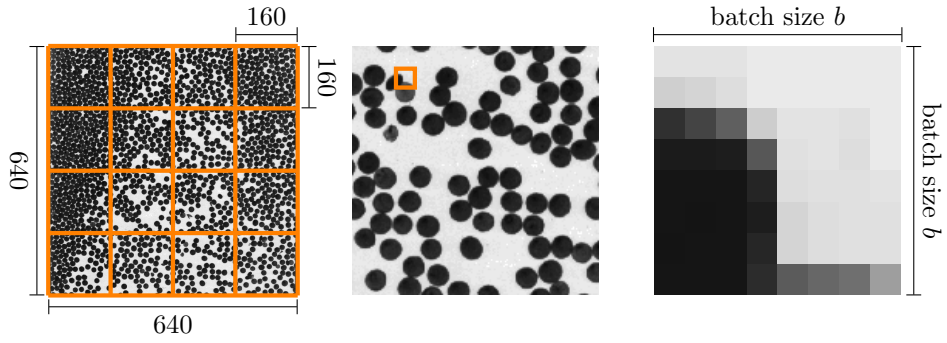

Fig. 3.2: Left to right: Creation of 160×160 pixels partial images from given imagery of size 640×640, example partial image and one example batch with a batch size $b = 8$.

of this code serves to enhance the reproducibility of our results and facilitate their comparison with those of other researchers in this field. However, we also incorporate a slicing technique, as explained below.

Our starting data set contains 12 images $I_{\text{orig}} \in \mathbb{R}^{640\times 640}$, which we want to extend by slicing the images. In doing this, we aim for two goals: First, we increase the number of elements in the data set. Second, working with smaller images will reduce computation time. By this motivation, we divide the images into 4×4 blocks equal in size, see Fig. 3.2 left. Each block, with a resolution of 160×160 pixels, will be saved as a separate image, yielding in total a new larger data set. This enlarged data set now contains 192 images and is used to learn the dictionary D.

We now pursue to explain the preprocessing step $\mathcal{P}\colon I \to W$. In the first step, we are randomly choosing 20 out of these 192 images to assemble the foundation for training our dictionary D. At this point, we actually need the enlarged data set. During the second step, the images I will be completely divided into small image batches $B_i \in \mathbb{R}^{b\times b}$, $i \in \{1, 2, \ldots, n_b\}$ of a resolution $b \times b$, as shown in Fig. 3.2 middle and right. Since our focus will now be on numerical computing rather than on interpretation as image batches, we will call B_i batch, b the batch size, and n_b is the number of batches in the image I. This dividing is not overlapping, and a single batch is visualized in Fig. 3.2 right.

Next, in the third step, we will concatenate these batches B_i to create the vector $w_i \in \mathbb{R}^{b^2}$.

$$B_i = [v_1, \ldots, v_b] \in \mathbb{R}^{b\times b} \quad \to \quad \left[v_1^T, \ldots, v_b^T\right]^T = w_i \in \mathbb{R}^{b^2} \tag{3.1}$$

Concatenating all n_b batches B_i of I and pinning them together will construct the matrix $W = [w_1, \ldots w_{n_b}] \in \mathbb{R}^{b^2\times n_b}$.

Finally, we have transformed the images $I \in \mathbb{R}^{160\times 160}$ into the matrix $W \in \mathbb{R}^{b^2\times n_b}$. We can reverse this process $\mathcal{P}^{-1}\colon W \to I$ to construct an image I from a matrix W. This is used to visualize the recovered images $w_i = Dx^{\text{opt}}$, $\forall i \in [1, n_b]$, where x^{opt} is the solution from (3.3).

3.2. Revisiting Sparse Coding. In accordance with Section 2, the K-SVD method is based on the sparse coding problem that may be formulated in general in terms of (2.3) and (2.4). After preprocessing, let us now reformulate them as one

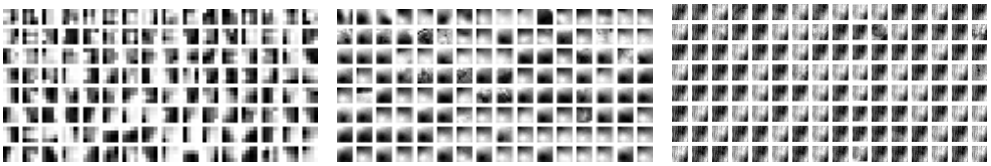

Fig. 4.1: Visualization of the three learned dictionaries. From left to right we have $b = 4, 8, 16$ and show D_4, D_8, D_{16}, respectively.

problem mainly used for learning as

$$\forall i \in [1, N] \quad \min_{D,\, x_i} \|w_i - Dx_i\|_2^2 \quad \text{w.r.t.} \quad \|x_i\|_0 \leq T_{\text{train}} \tag{3.2}$$

and one for testing a computed reconstruction:

$$\forall i \in [1, n_b] \quad x^{\text{opt}} = \arg\min_{x_i} \|w_i - Dx_i\|_2^2 \quad \text{w.r.t.} \quad \|x_i\|_0 \leq T_{\text{test}} \tag{3.3}$$

3.3. Solving the minimization problem. Solving (3.2) will follow as shown in [2, Figure 2], which we will briefly recall now. In the sparse coding stage, the orthogonal matching pursuit algorithm is employed to solve (3.2) only for x_i. In the dictionary update stage, we can use the solution of the previous stage to enhance the dictionary with (2.6). This iterative process of using D to find a better x and then use x to find a better D is done, until the process converges.

To provide a profound understanding of the dictionary update process, we first address the initialization of D. We use $K \in \mathbb{N}$ random batches B_i from our 20 images used for training and normalize ($\|B_i\|_2 = 1$) them. After concatenating all B_i the dimension of the dictionary will be $D \in \mathbb{R}^{b^2 \times K}$. An additional part of the updating stage, see Section 2.2, is, to control if the atoms in the dictionary are used or not, i.e. all x^{opt} have a zero entry at a certain index. If we do not use an atom, we simply replace it with another, random and already not in use, normalized concatenated batch.

4. Experimental Results and Discussion. Let us start with the dictionaries, and continue with the recovery of selected images. After discussing these, we will proceed with a parameter study and the impact of the texture on the recovery process.

4.1. Learning the Dictionaries. We learn the dictionaries $D_b \in \mathbb{R}^{b^2 \times K}$ for different batch sizes $b = \{4, 8, 16\}$. The batch size of $b = 4$ can be interpreted as the minimum batch size, since $b = 2$ would be too small, and we end up in learning almost every pixel by itself. Doubling the batch size to $b = 8$, and again to get $b = 16$, appears to be a natural choice, since it keeps divisibility to the image resolution. Other batch sizes are possible, but are not in the focus of this paper. With D_b, we will denote the learned dictionaries corresponding to batch size. The number of atoms in the dictionary will be set to $K = 128$, and we set $T_{\text{train}} = 5$. The learned dictionaries can be seen in Fig. 4.1, and will be used to recover the images.

Inspecting these dictionaries, we notice, that with an increasing batch size b, the atoms more and more look like each other.

4.2. Generalization Experiment. After learning the dictionary D_b, we can solve (3.3) to recover an image, via

$$I_{\text{rec}} = \mathcal{P}^{-1}(W_{\text{rec}}) \quad \text{with} \quad W_{\text{rec}} = [w_1^{\text{rec}}, \ldots, w_{n_b}^{\text{rec}}] \quad \text{and} \quad w_{n_b}^{\text{rec}} = D_b x^{\text{opt}} \tag{4.1}$$

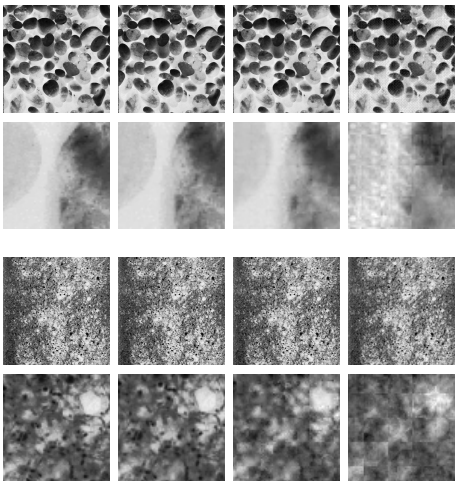

(a) Recovery of the 640×640 images D30 and D73 from the Brodatz data set.

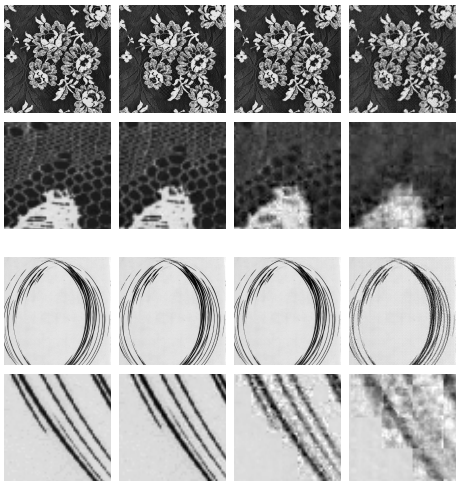

(b) Recovery of the 640×640 non-subset images D42 and D44 from the Brodatz data set.

Fig. 4.2: From left to right, we present the original image first, followed by recovery using D_4, D_8 and D_{16}, respectively. In the first and third row, we see the images in total, and the rows two and four are showing zoomed in versions of the recoveries.

For this experiment, we have chosen $T_{\text{rec}} = 10$. The results can be seen in Fig. 4.2. On the left (cf. Fig. 4.2a) we present the results of two images (D30 and D73) that were part of the subset and therefore part of the training. The right images (cf. Fig. 4.2b) are the results of images (D42 and D44) not part of the training subset. In the first and third row of Fig. 4.2, we show the image in the original resolution of 640×640 pixels. In the rows two and four, we are presenting a zoomed part of the image above. The first column is always presenting the original image. The columns two, three, and four reveal the recoveries using D_4, D_8 and D_{16}, in this order.

Visual inspection of Fig. 4.2 reveals that using D_4 (column 2 and 6) will recover the images almost perfectly. The recovery using D_8 (column 3 and 7) works pretty well, if only focusing on the full resolution image. Examining the zoomed parts, we notice that block-like artefacts emerge. In recovery with D_{16}, these artefacts are even more dominant, even in the full resolution image.

We will use the mean squared error, $\text{MSE} = \|I - I_{\text{rec}}\|_2^2/m$ with m the number

b	D30	D73	avg. of subset	D42	D44
4	$2.1 \cdot 10^{-3}$	$3.8 \cdot 10^{-3}$	$3.85 \cdot 10^{-3}$	$6.2 \cdot 10^{-3}$	$3.2 \cdot 10^{-3}$
8	$1.07 \cdot 10^{-2}$	$2.32 \cdot 10^{-2}$	$2.44\bar{3} \cdot 10^{-2}$	$3.55 \cdot 10^{-2}$	$2.36 \cdot 10^{-2}$
16	$2.73 \cdot 10^{-2}$	$4.25 \cdot 10^{-2}$	$4.9\bar{3} \cdot 10^{-2}$	$5.72 \cdot 10^{-2}$	$4.44 \cdot 10^{-2}$

Table 4.1: The mean squared error (MSE) of different images (part or not part of the subset) and the average of our subset of the Brodatz data set to different batch sizes b.

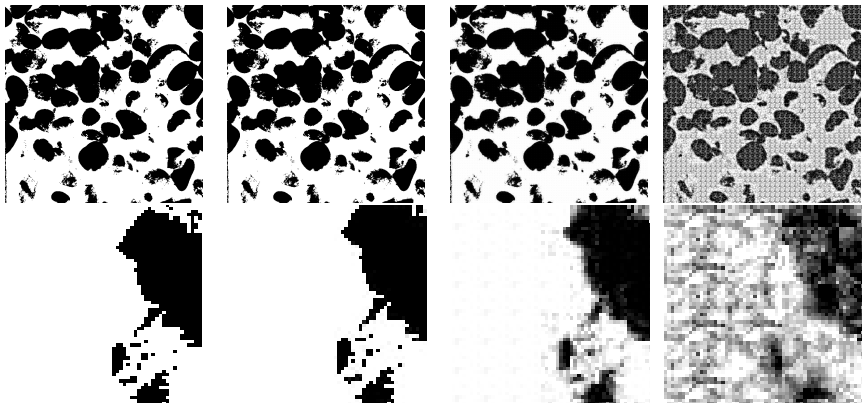

Fig. 4.3: From left to right, we present the original image first, and the recovery using D_4, D_8 and D_{16}. From top to bottom row, we see the image in total, and a zoomed version.

of pixels in the image, to quantify the reconstruction quality of the recovered image. The MSE values for the images in Fig. 4.2 are listed in Table 4.1. There we see, that if we switch from a batch size $b = 4$ to $b = 8$, we will increase the error by almost a power of ten. Then again, switching from $b = 8$ to $b = 16$ only roughly doubles the error. Generalizing from images that are part of our training set, to images that are not, seems to have no significant impact on recovery quality.

The number of details/texture in an image appears to be impactful on MSE and the recovery quality. The bottom image in Fig. 4.2a (D73) and the top image in Fig. 4.2b (D42) are highly textured images and have higher MSE values than the other two, less detailed, images in Fig. 4.2.

4.3. Binary Image Experiment. We ended the last section with the hypothesis, that highly textured images produce larger MSE values. But first, we have to mention that the Brodatz images contain some visually not apparent noise that could influence the observed MSE values, as the method will attempt to recover it.

To study this issue, we created a binary (black and white) version of our training dataset. Then we learned a dictionary in the same way as before. No parameters were changed or adjusted. From the learning process we obtained the three dictionaries D_4^{bw}, D_8^{bw} and D_{16}^{bw}.

An example of original image and recoveries can be seen in Fig. 4.3, keeping the order of Fig. 4.2. We notice that the recovery using D_4^{bw} leads to an almost perfect recovery. However, there are still problems with the details. i.e. in the top-right corner within the zoomed frame of the original image. There we notice a hook-like structure, that vanishes during the recovery process.

Considering the recovery using D_8^{bw}, we notice that the full-size image still looks very similar to the original image, on one hand. On the other hand, in the zoomed image, a blurring occurs that gets even more dominant in the recovery with D_{16}^{bw}. The latter recovery can no longer be visually declared as a black-and-white image. This gray blurring comes from the normalization while learning the dictionary. Therefore, using only binary images will not lead to a binary or non-noise creating dictionary.

Computing the MSE for the recovered images, we get MSE $= 1.6891 \cdot 10^{-5}$ for

Fig. 4.4: The difference between the original black-and-white image (D30) and recovery using D_8^{bw}, where values above/below zero were indicated with blue/red dots. The left image shows the total, and in the right image we show a zoomed part.

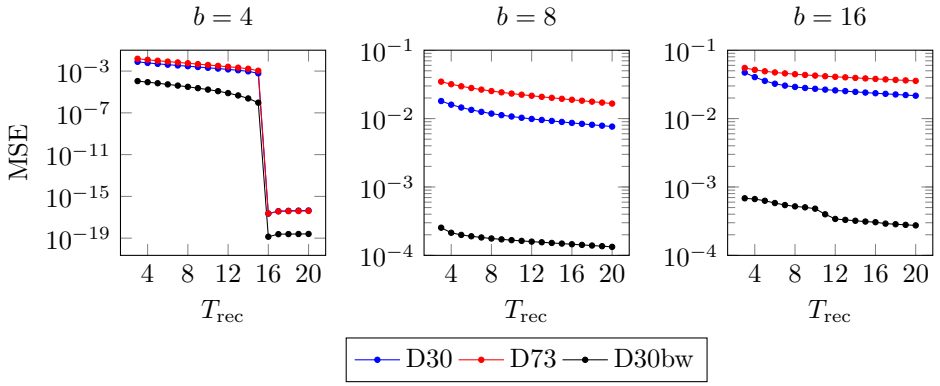

Fig. 4.5: The MSE between original and recovered image, with different values for T_{rec}. From left to right we recovered with $b = 4$, $b = 8$, and $b = 16$. The blue line indicates the D30 image, the red line belongs to the image D73, and the black denotes the black-and-white version of D30.

$b = 4$, $\mathrm{MSE} = 1.6699 \cdot 10^{-4}$ for $b = 8$, and $\mathrm{MSE} = 4.8149 \cdot 10^{-4}$ for $b = 16$. We notice that the MSE belonging to D_{16}^{bw} is still smaller than the MSE of the gray valued recovery with D_4.

In Fig. 4.4, we plot the difference between the original image in black-and-white and the recovery based on D_8^{bw}. On the right plot, we present a zoomed in image. The zoomed part was indicated left plot with a black square. Red dots indicate negative and blue dots a positive difference between the original and the recovery. The plots indicate that all errors occur on the edges of the texture.

4.4. Studying the Parameter T_{rec}. In the previous experiments, we always fixed $T_{\mathrm{rec}} = 10$. This parameter controls the number of used atoms in the recovery. To study its influence, we compute the MSE of the recovery obtained with different values of $T_{\mathrm{rec}} \in [3, 20]$ in (3.3). The results are visualized in Fig. 4.5.

In this figure, we gave each batch a plot. From left to right, we present the MSE of the recovery using D_b with $b = 4$, $b = 8$ and $b = 16$. The blue line indicates the D30 image (cf. Fig. 4.2a top), the red line belongs to the image D73 (cf. Fig. 4.2a

bottom), and the black denotes the black-and-white version of D30 (cf. Fig. 4.3).

As a main observation, the batch size seems to have a bigger impact on increasing the recovery quality, than increasing the number of used atoms T_{rec}. However, reducing the batch size will lead to an increase in computation time. In the end, we have to balance low MSE versus computation time.

In the left plot ($b = 4$) we see a considerable drop in the MSE for $T_{\text{rec}} \geq 16$. The same drop could be noticed if we use $T_{\text{rec}} \geq 64$ or $T_{\text{rec}} \geq 256$ for 8×8 and 16×16 batches, respectively. Thus, using values $T_{\text{rec}} \geq b^2$ appears to be beneficial in terms of the MSE, but they are not a reasonable option for the K-SVD procedure itself.

5. Conclusion and Future Work. Concerning recovery of highly textured images, we found that the biggest part in reconstruction error is by the recovery of edges. Additionally, we have shown that increasing the number of used atoms has a limited effect on increasing the quality of the recovered image.

Acknowledgments. The authors acknowledge funding of the work by the DLR project AIMS:AIDIA with the funding number 50WK2270F.

REFERENCES

[1] Brodatz's texture database. website: `https://www.ux.uis.no/~tranden/brodatz.html`.
[2] M. Aharon, M. Elad, and A. Bruckstein. K-SVD: An algorithm for designing overcomplete dictionaries for sparse representation. *IEEE Transactions on Signal Processing*, 54(11):4311–4322, November 2006.
[3] Michal Aharon, Michael Elad, and Alfred M. Bruckstein. On the uniqueness of overcomplete dictionaries, and a practical way to retrieve them. *Linear Algebra and its Applications*, 416(1):48–67, 2006. Special Issue devoted to the Haifa 2005 conference on matrix theory.
[4] Dennis Bontempi. KSVD. GitHub: `https://github.com/denbonte/KSVD`, 2018.
[5] Phil Brodatz. *Textures: A Photographic Album for Artists and Designers*. Dover books on art, graphic art, handicrafts. Dover Publications, 1966.
[6] Kai Cao, Eryun Liu, and Anil K Jain. Segmentation and enhancement of latent fingerprints: A coarse to fine ridgestructure dictionary. *IEEE transactions on pattern analysis and machine intelligence*, 36(9):1847–1859, 2014.
[7] Michael Elad. *Sparse and redundant representations: from theory to applications in signal and image processing*. Springer Science & Business Media, 2010.
[8] Kjersti Engan, Sven Ole Aase, and John Håkon Husøy. Multi-frame compression: Theory and design. *Signal Processing*, 80(10):2121–2140, 2000.
[9] Allen Gersho and Robert M Gray. *Vector quantization and signal compression*, volume 159. Springer Science & Business Media, 2012.
[10] Raja Giryes and Michael Elad. Sparsity-based poisson denoising with dictionary learning. *IEEE Transactions on Image Processing*, 23(12):5057–5069, 2014.
[11] Sylvain Lesage, Rémi Gribonval, Frédéric Bimbot, and Laurent Benaroya. Learning unions of orthonormal bases with thresholded singular value decomposition. In *Proceedings.(ICASSP'05). IEEE International Conference on Acoustics, Speech, and Signal Processing, 2005.*, volume 5, pages v–293. IEEE, 2005.
[12] Michael S Lewicki and Terrence J Sejnowski. Learning overcomplete representations. *Neural computation*, 12(2):337–365, 2000.
[13] Liyan Ma, Lionel Moisan, Jian Yu, and Tieyong Zeng. A dictionary learning approach for poisson image deblurring. *IEEE Transactions on medical imaging*, 32(7):1277–1289, 2013.
[14] Bruno A Olshausen and David J Field. Emergence of simple-cell receptive field properties by learning a sparse code for natural images. *Nature*, 381(6583):607–609, 1996.
[15] Ron Rubinstein, Michael Zibulevsky, and Michael Elad. Efficient Implementation of the K-SVD Algorithm Using Batch Orthogonal Matching Pursuit. *CS Technion*, 40, April 2008.
[16] Joel Aaron Tropp. *Topics in sparse approximation*. The University of Texas at Austin, 2004.
[17] Shiming Xiang, Gaofeng Meng, Ying Wang, Chunhong Pan, and Changshui Zhang. Image deblurring with coupled dictionary learning. *International Journal of Computer Vision*, 114:248–271, 2015.
[18] Qiang Zhang and Baoxin Li. *Dictionary learning in visual computing*. Springer Nature, 2022.